Journal of Solid State Chemistry 182 (2009) 827–835

Contents lists available at ScienceDirect

Journal of Solid State Chemistry

journal homepage: www.elsevier.com/locate/jssc

Photoluminescence and Raman spectroscopy studies on polyaniline/PbI_2 composite

M. Baibarac [a,*], I. Baltog [a], S. Lefrant [b]

[a] National Institute of Materials Physics, Laboratory Optics and Spectroscopy, Bucharest-Magurele, MG-7, R77125, Romania
[b] Institut des Materiaux "Jean Rouxel", 2 rue de la Houssinière, B.P. 32229, 44322 Nantes Cedex 3, France

ARTICLE INFO

Article history:
Received 27 August 2008
Received in revised form
29 December 2008
Accepted 1 January 2009
Available online 20 January 2009

Keywords:
Hybrid materials
Lead iodide
Conducting polymers
Charge collector

ABSTRACT

Functionalization of PbI_2 with conjugated polymers (polyaniline-emeraldine base (PANI-EB) or polyaniline-emeraldine salt (PANI-ES)) is demonstrated by Raman and luminescence studies. PbI_2/PANI hybrid material was prepared by electrochemical polymerization of aniline onto the PbI_2 modified Pt electrode and mechanico-chemical reaction between the two constituents. PANI interacting with the PbI_2 gives rise to new Raman bands at 80, 144 and 170 cm^{-1}. First line reveals the formation of "stacking faults" that disrupt the I–Pb–I layers stacking along the *c* axis by the insertion of polymer molecules. The bands at 144 and 170 cm^{-1} are attributed to the vibrational mode associated with Pb-NHR''_2 ($R'' = C_6H_4$) bond. The functionalization of PbI_2 with PANI-EB brings forth the PANI-ES form. Depending on the semiconducting (PANI-EB) or conducting (PANI-ES) properties of the polymer in the PbI_2/PANI intercalated material, a partial or total collection of the charges generated under band to band irradiation is revealed by photoluminescence studies.

1. Introduction

In the last years, a special attention has been given to the basic and applicative research of organic/inorganic hybrid materials. Thus, detailed studies have been performed on materials such as: (i) isolated or conducting polymers functionalized carbon nanoparticles (carbon nanotubes, fullerenes) [1], (ii) composites achieved from polymers or biopolymers with different oxides (SiO_2, Al_2O_3, V_2O_5, etc. Refs. [2–5]) or metallic nanostructures (for example: poly o-phenylene diamine/Au [3], etc.), (iii) inorganic semiconductors of the type CdS, CdSe, ZnS, ZnO, TiO_2 produced in the presence of polymers (see Refs. [6,7]). For these hybrid materials, different applications have been reported in the field of sensors, storage energy, biomedical and textile industry. New applications in opto-electronics are envisaged for hybrid compounds based on the intercalated layered structures. This family of solids in which the atoms are arranged successively in layers characterized by strong intralayer chemical bonding and weak interlayer van der Waals interactions has attracted much interest for fundamental research and technological applications. This is motivated by the ability to model new properties resulting from the intercalation between layers of foreign atoms, ions and molecules. Among layered materials a good example is PbI_2, which has, as a rigid structurally repeated unit, an I–Pb–I layer of 0.7 nm thickness arranged successively and perpendicularly along the *c* axis [8,9]. Lead iodide, as a direct band gap semiconductor of about 2.5 eV, shows at low temperature a strong photoluminescence (PL) originating from exciton recombination and trapped electrons–hole pairs which have been formed by the band-to-band irradiation [10]. Intercalation produces an increase in the *c* axis parameter as a result of the destruction of stacking continuity of layers along the *c* axis. It is similar to a polytypic transformation which results in variations in the sequences of stacking layers along the layer normal to the hexagonal *c* axis [11]. In this sense Fig. 1 is illustrative, it shows that the PbI_2 single crystal extends along the *c* axis as result of the intercalation of pyridine. The stacking faults produced in this way detach closed packed I–pb–I layers of limited thickness. As a general rule, an intercalated structure exhibits an increased degree of disorder, an alternation of intercalated and non-intercalated regions. The "flaky" structure generated in this way of intercalated PbI_2 behaves similarly as the PbI_2 crystalline powder, it being characterized by a high density of surface defects where the largest part of the trapping centers (iodine vacancies, Pb+ ions, dislocations) for excitons and free carriers, are localized. Due to this fact in the PL spectrum at low temperature (liquid nitrogen temperature—LNT) of PbI_2, as intercalated single crystal or crystalline powder, at least two emission bands are detected: one originating from the radiative recombination of cationic excitons, including self-trapped excitons, and the other stemming from the radiative recombination of the trapped carriers, labeled the G band [12]. Thus, the G band can be considered a measure of the radiative recombination yield of

* Corresponding author. Fax:+40 21 3690177.
E-mail address: barac@infim.ro (M. Baibarac).

0022-4596/$ - see front matter © 2009 Elsevier Inc. All rights reserved.
doi:10.1016/j.jssc.2009.01.007

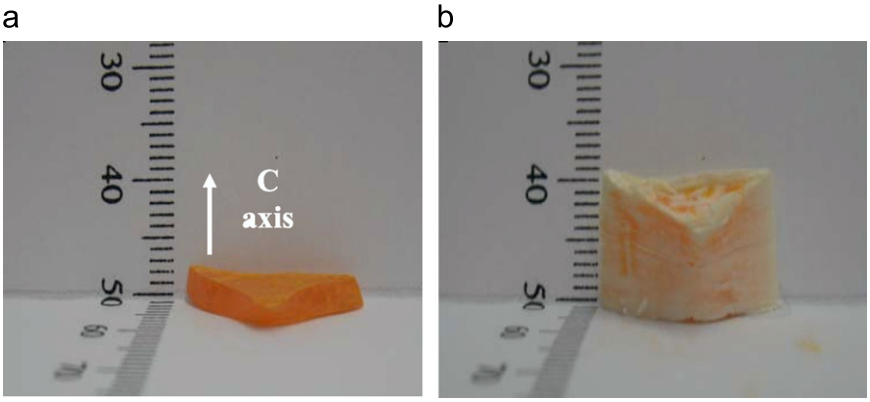

Fig. 1. Experimental illustration of the extending along the *c* axis of a PbI_2 single crystal by an intercalation process. In (a) is shown a crystal slide cleaved from a Bridgman-grown PbI_2 crystal ingot and in (b) the same sample intercalated with pyridine obtained after an exposure for 24 h in a saturated atmosphere of pyridine.

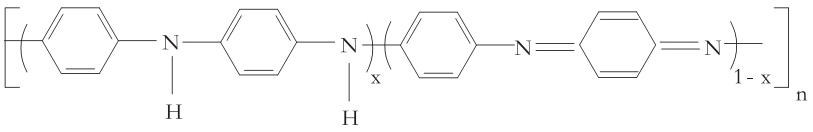

Scheme 1.

trapped carriers produced by band-to-band irradiation. In such a scenario, if the carriers are collected before their trapping, the intensity of the G band will decrease in comparison with the excitonic emission band. Hereinafer, one prove a collecting process of the charges (electrons and holes) generated by band-to-band irradiation in the composite PbI_2/polyaniline (PANI).

The intercalation of guest molecules between the iodine atomic planes perturbes the iodine orbitals so that a reduction of the contribution of the 5*p* states of I^- ions to the uppermost valence band appears. This induces a weakness in the interaction between the lead ion and iodine electron within a layer and the transition $1S_0 \rightarrow 3P_1$ of the Pb^{2+} ions shifts towards higher energies. A shift of the cationic absorption band to higher energies was indeed observed in PbI_2 intercalated with a variety of Lewis base ligands, including hydrazine [13], pyridine [14,15], ammonia and aniline (ANI) [16–20]. In order to the determination of the interaction type between host matrice (PbI_2) and guest molecules (ANI, PANI, etc.) experimental techniques as Raman scattering, PL FTIR spectroscopy, X-ray diffraction and nuclear quadrupole resonance were used. Using the last three methods, in Ref. [20] is shown that the intercalation of PbI_2 with ANI or PANI leads to an increased inter-plane distance of 1.26 nm. Similarly, Fig. 1 shows an expansion of the crystal along the *c* axis when PbI_2 was intercalated with pyridine. The Raman spectrum of pyridine intercalated PbI_2 is complex and entirely different from that of the pristine material. It reveals an orthorhombic structure characterized by the appearance of a number of sharp low-frequency Raman lines below 100 cm^{-1}. The most revealing is a new band peaking at about 88 cm^{-1} that is associated with the formation of staking faults that disrupt the I–Pb–I layers stacking along the *c* axis by the insertion of pyridine molecules [21]. It is important to notice that the same band is observed also in un-intercalated crystals which were previously submitted to a polytypic transformation achieved at 400–600 K [22,23]. It was attributed to the interface phonons which propagate along the planar defects produced by staking faults [22].

In the light of these observations, this paper has as the aim to provide new information concerning the intercalation of PbI_2 with PANI in its two forms, emeraldine base (PANI-EB) and emeraldine salt (PANI-ES). In comparison with Ref. [20], in this paper the intercalated materials were prepared by: (i) electrochemical polymerization of ANI on the PbI_2 modified Pt electrode and (ii) mechanico-chemical route. The mechanico-chemical reaction evolves by a mechanical motion/energy-controlled chemical process [24]. In the present case, the solid-phase mechanico-chemical reaction occurs between PbI_2 crystalline powder and PANI-EB or PANI-ES. To a better understanding of the interactions invoked below a brief review of the molecular structure of PANI is shown in following. PANI is a polymer whose repeating unit contains two entities with different relative weights (Scheme 1).

The reduced ($x = 1$) and oxidized ($x = 0$) forms are known under the name of leucomeraldine base (LB) and pernigraniline base (PB), respectively. The intermediate state ($x = 0.5$), in which the oxidation and reduced degrees of PANI are equal to each other, is known as PANI-EB. In the case of the electrochemical synthesis, the method often used is the cyclic voltammetry, the aqueous acidic medium being frequently H_2SO_4 or HCl. The reaction products correspond to the doped states of PANI known as PANI-ES, LS and PS [25]. *A priori*, the two synthesis methods, namely the electrochemical polymerization and the mechanico-chemical reactions, must lead to hybrid compounds with similar properties.

The intercalation of the PANI molecules between the crystalline I–Pb–I layers can be governed by: (i) weak forces associated to physical adsorption or (ii) strong forces resulting from charge transfer between the two constituents, of organic (ANI or PANI) and inorganic (PbI_2 crystal) nature. Using Raman spectroscopy, one proposes an intercalation mechanism of PbI_2 with PANI. Beside, PL studies carried out on the PANI/PbI_2 composite under band-to-band irradiation shows evidence of a charge collecting process.

2. Experimental section

Slides of PbI_2 have been cleaved from a single crystal ingot of 5 cm length and 2 cm diameter, which was grown by the Bridgman method from chemically purified raw material. The

crystal growth takes place by a controlled freezing process under a temperature gradient. Because in the Bridgman-grown PbI_2 crystals the most frequently observed polytypes are 2H and 4H , the transformation of the 2H in 4H polytype was obtained by a thermal annealing at 420 k [26]. This inter-polytype transformation was monitored by the Raman line at 76 cm^{-1}, which attains its maximum for the 4h polytype.

Two routes were used to prepare the PANI/PbI_2 hybrid material. The first one consists of the electrochemical polymerization of ANI on the PbI_2 modified Pt electrode via cyclic voltammetry. For this, one used a conventional three-electrode one-compartment cell, having as working electrode a PbI_2 modified Pt support and a spiral Pt wire as auxiliary electrode. The reference electrode was a saturated calomel electrode (SCE). The working electrode was immersed into an aqueous solution of 0.5 M HCl or 0.5 M H_2SO_4 and 0.05 M ANI. All compounds were purchased from Aldrich-Sigma. The PANI films were obtained with a sweep rate of 25 mV s^{-1} between −100 and +900 mV vs. SCE. In this way, we obtained PbI_2 samples intercalated with a conducting polymer of the type PANI-ES. As is well known, the interaction of PANI-ES with a basic solution leads to a de-doping process of conducting polymer resulting in a PANI-EB [27]. Similarly, in the present paper a composite material of the type PbI_2/PANI-EB, was obtained by the interaction of the PbI_2/PANI-ES samples, electrochemically prepared, with an aqueous 1 M NH_4OH solution for 5 min. The electrochemical polymerization of ANI on the PbI_2 modified Pt electrode was carried out using a potentiostat/galvanostat type VOLTALAB 80 from Radiometer Analytical. Gravimetric analysis of the PbI_2 modified Pt electrode, before and after electrochemical polymerization of ANI, shows that the mass ratio of PANI-ES: PbI_2 is of ca. 0.05 and 0.12, when 25 and 50 cyclic voltammograms, respectively, was carried out. In these two cases, the percentage mass of polymer intercalated within the PbI_2 is estimated to be of ca. 4.8% and 10.7%, respectively.

The second route consists of a mechanico-chemical reaction by which a crystalline powder of PbI_2 mixed ca. 5 and 10 wt% polymer in the un-doped (PANI-EB) or doped state (PANI-ES) was compressed non-hydrostatically for ca. 2 min at 0.58 GPa. The PANI was prepared by a typical procedure consisting of a mixture of ANI [(1.022 g, 1.09×10^{-2} mol) in 25 ml of 0.5 M HCl] and $K_2Cr_2O_7$ [(0.56 g, 1.9×10^{-3} mol) in 25 ml of 0.5 M HCl] solutions left standing under ultrasonications for 2 h at 0 °C. The resulting green suspension, indicating the formation of PANI in its ES form, was filtered and the filter cake was washed with 1000 ml of deionized water [25]. A part was dried under vacuum at room temperature until constant mass. Another part, stirred in ammonium hydroxide solution (500 ml 1 M NH_4OH) for 1 h, transforms the salt form, i.e., (PANI-ES) into the base form, i.e., (PANI-EB). After filtering, the oligomers were extracted with 400 ml of acetonitrile (CH_3CN) until the solvent was colorless and the remaining powder was dried as in the case of PANI-ES.

Raman studies have been carried out at the wavelength excitation of 1064 nm using a FT Raman Bruker RFS 100 spectrophotometer.

PL spectra at LNT under wavelength excitation of 460 nm and in right angle geometry have been obtained with a Horiba Jobin Yvon Fluorolog-3 spectrometer, model FL 3-22.

3. Results and discussions

Fig. 2 shows the cyclic voltammograms of PANI deposited on the Pt alone support and PbI_2 modified Pt electrode in the

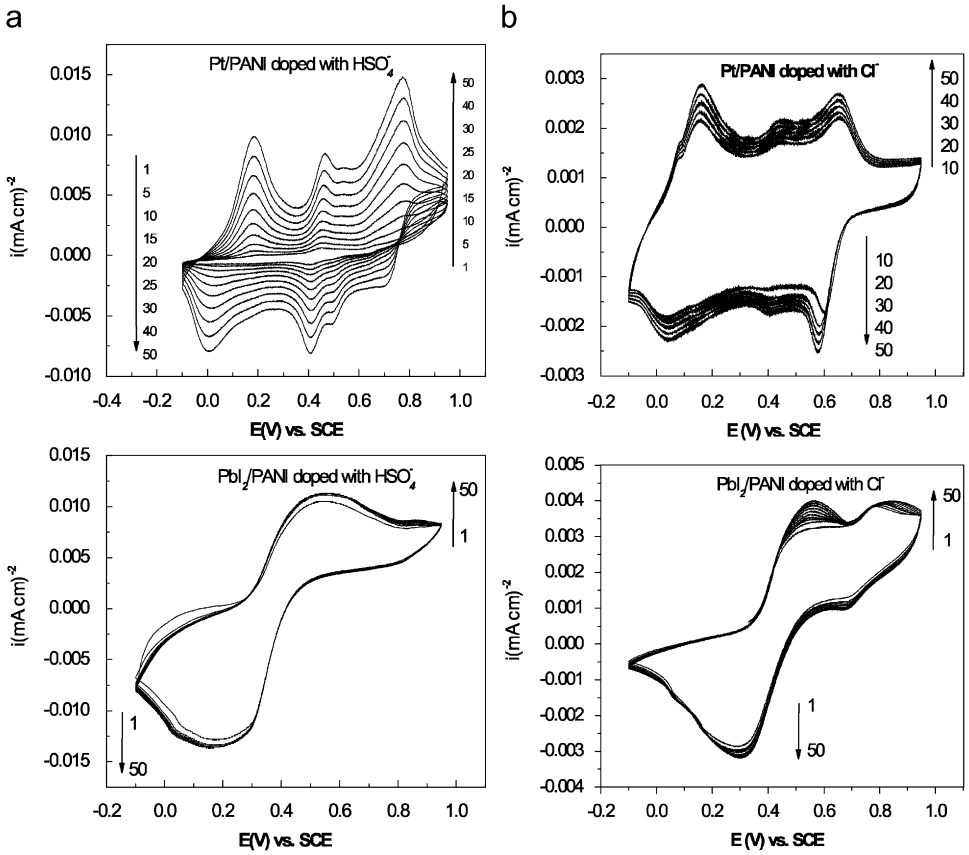

Fig. 2. Cyclic voltammograms of the electrochemical polymerization of aniline in aqueous 0.5 M H_2SO_4 and 0.5 M HCl media carried out on the Pt support and PbI_2 modified Pt electrode in the potential range (−100; +900) mV vs. SCE with the sweep rate of 25 mV s^{-1}.

presence of aqueous 0.5 M H_2SO_4 or 0.5 M HCl solutions. It is well known that cyclic voltammograms of PANI recorded in aqueous acidic media usually show two redox couples associated with interconversion between leucoemeraldine and emeraldine (first couple) and between emeraldine and pernigraniline (the second couple) [28]. An analysis of Fig. 1a shows that, in the case of PANI electrogenerated in the 0.5 M H_2SO_4 medium on the Pt electrode, the three oxidation maxima are situated at ca. 184, 464 and 774 mV vs. SCE and the corresponding reduction maxima are localized at ca. 4, 405 and 691 mV, respectively. On the same Pt electrode, when the electro generation of PANI is made in an aqueous 0.5 M HCl solution (Fig. 2b), one observes small changes in the position of oxidation and reduction maxima. Thus, the anodic maxima are at 161, 436 and 653 mV while their cathodic replicas are localized at 37, 405 and 579 mV vs. SCE. Things are different when the electrochemical polymerization of ANI takes place on the PbI_2 modified Pt electrode. In this context, depending on the acid medium used, one observes for H_2SO_4 only one redox couple with the oxidation and reduction maxima at 541 and 169 mV vs. SCE, respectively, while for HCl, two redox couples appear with the oxidation maxima at 558 and 789 mV and the reduction maxima at ca. 306 and 681 mV vs. SCE. In this stage of the investigation, the question arises from the above electrochemical process if a hybrid material of the type PbI_2/ANI or a PANI/PbI_2 composite is created? Before answering this question, we note that a common characteristic of voltammograms shown in Fig. 2 consists of the growing of the intensity of the oxidation and reduction maxima with the increase of the voltammetric cycles number. A discussion about the reversible or irreversible character of the electrochemical transformation can be done referring to the equations:

$$\Delta E = E_{p,a} - E_{p,c} = 0.58/n \quad (1)$$

$$E_p - E_p/2 = 0.59/n \quad (2)$$

where ΔE is the potential of separation of the anodic and cathodic peaks, $E_{p,a}$ and $E_{p,c}$ correspond to anodic and cathodic peak potentials, respectively, $E_{p/2}$ is the half wave potential and n is the number of transferred electrons. In the case of a reversible charge transfer involving one electron and no coupled chemical reaction, the value of ΔE and the peak width are equal to ca. 60 mV and the ratio of the cathodic to anodic peak currents $i_{pc}/i_{pa} \approx 1$. Based on this and taking into account results shown in Fig. 2, we conclude that regardless of the type of acid, when a PbI_2 modified Pt electrode is used, the oxidation–reduction reactions which have evolved in the potential range (−100; +900) mV vs. SCE have an irreversible character. This is due to the deposition of PANI-ES on the PbI_2 modified Pt electrode. This statement is sustained by Raman spectroscopic studies performed at the excitation wavelengths of 1064 nm, Fig. 3. The curves 1 and 4 from Fig. 3 represent the Raman spectra of PbI_2 and PANI-ES. In the spectral range 50–200 cm^{-1}, PbI_2 shows a complex band composed from the Raman lines with the maxima at 75, 96, 112, 144 and 160 cm^{-1} which can be attributed the vibration modes E_2^1, A_1^1, A_1^2, $2E_2^1$ and $2E_1^1$, respectively, all being characteristic of the poly-type 4H–PbI_2 crystal [29,30]. According to the spectrum 4 from Fig. 3, the main Raman lines of PANI-ES are found in the spectral range 1000–1650 cm^{-1}. The lines peaking at ca. 1170, 1240, 1330–1370, 1500, 1573 and 1625 cm^{-1}, are associated to the following vibration modes: C–H bending (B)-Ag mode, C–C stretch. (B)+ring def., protonated structure, C═N stretch. +C–H bending (B), C═C stretch. (Q)+C–C stretch. (B) and C–C stretch. (B) +C–H bending (B) (B = benzene ring, Q = quinoid ring), respectively [31]. Increasing the number of cycles recorded on a PbI_2 modified Pt electrode, from 25 to 50 (spectra 2 and 3 in Fig. 3), one observes the appearance of all specific vibrations of PANI-ES. In the low-

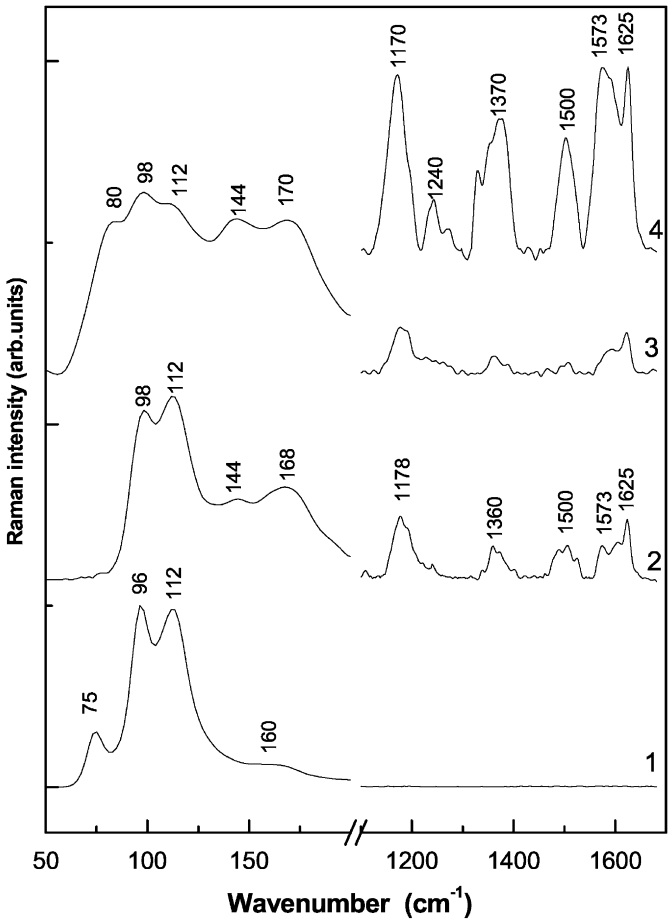

Fig. 3. Raman spectra at $\lambda_{exc} = 1064$ nm recorded on the PbI_2 modified Pt electrode in the initial state (1) and after the electrochemical deposition of PANI during of 25 (2) and 50 (3) cyclic voltammograms. Spectrum 4 corresponds to the PANI-ES film deposited on the Pt support.

frequency spectral range, where are situated the Raman lines of PbI_2, a gradual increase of the Raman lines intensity at 140 and 170 cm^{-1} is observed. Thus, after the 50 cycles, the ratio between the intensities of Raman lines situated at 98–112 and 144–170 cm^{-1} change from 10:1 to 1:1. At the first sight, the enhancement of the Raman lines at 144 and 170 cm^{-1} can be interpreted as a result of an intercalation process of the PbI_2 crystal with PANI-ES. If this is correct, then the same lines should be seen in the case of the intercalation with other molecules. A good example is the case of the PbI_2 crystal intercalated with ANI. Very few studies have been dedicated to this subject.[16,18,20] According to Ref. [16], by the appearance of the strong Raman lines at 996, 1028 and 1600 cm^{-1}, have confirmed the presence of ANI in the interlayer space of PbI_2 when an increase of 0.5 eV of the optical band gap was reported. The published data reports only the presence of ANI in the PbI_2/ANI compound, but do not give any information about how the Raman spectrum of PbI_2 changes. Then, we tried to complete this information by the following. The hybrid material lead iodide/ANI (PbI_2/ANI) has been obtained by the immersion for 24 h of a crystalline PbI_2 sample of ca. 0.1 g in ca. 0.2 ml ANI. Its Raman spectrum is presented in Fig. 4 where one observes that the line at 173 cm^{-1} is strongly enhanced. On the same figure, we recognize the Raman lines of ANI at ca. 391, 532, 620, 815, 996–1030, 1154–1178, 1280 and 1602 cm^{-1} which are associated with the vibration modes C–C–C out of plane bending, C–C–C in plane bending, C_6–H out of plane bending, NH_2 rock. +C–H in plane bending, C–C

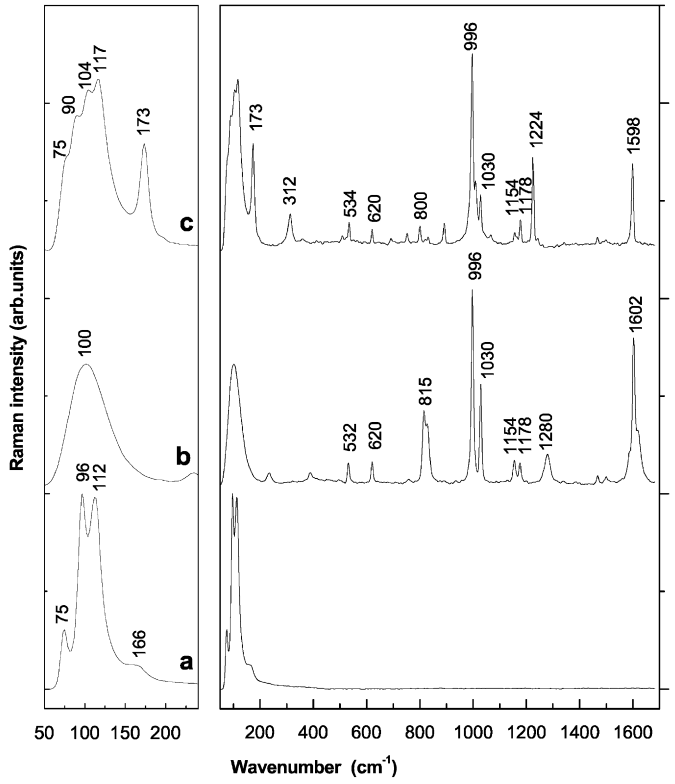

Fig. 4. Raman spectra at $\lambda_{exc} = 1064$ nm of: (a) crystalline PbI_2 powder, (b) aniline and (c) PbI_2 intercalated with aniline.

stretching+C–H in plane bending, C–C stretching+C–NH_2 bending and NH_2 scissoring+C–C stretching [32]. *A priori,* an intercalation process can be generated by physical or chemical mechanisms. In the former case, when the penetration between the atomic I–Pb–I layers is governed by a diffusion process, the layer structure is preserved so that the Raman spectrum of the final compound appears as a sum of the Raman spectra of host structure and guest molecules. The absence of new Raman lines is a proof of this mechanism. In the case of the chemical mechanism, by the interactions between the host structure and guest molecules, one obtains new compounds of different morphology, crystalline structure and composition. Obviously, the Raman spectrum of the new compound will reveal significant modifications of the Raman spectra of the two constituents. Thus, in comparison with the Raman spectrum of PbI_2 (curve a, Fig. 4), spectrum c in Fig. 4 shows the formation of a complex band covering the spectral range 50–250 cm^{-1} which in the final stage reveals lines localized at ca. 75, 90, 104, 117 and 173 cm^{-1}. the Raman line at 96 and 112 cm^{-1} observed in the Raman spectrum of PbI_2 are shifted to 104 and 117 cm^{-1} and indicates a chemical interaction between PbI_2 and ANI. The penetration into PbI_2 layer structure of ANI molecules disrupts the stacking sequence continuity of I–pb–I layers along the *c* axis by the formation of staking faults whose Raman signature is revealed by the line at ca. 90 cm^{-1}. Recently, similar results have been reported for the PbI_2 crystal intercalated with pyridine [15]. The appearance of the new Raman line at ca. 312 cm^{-1} has some significance; it may mark the formation of another material with a different morphological form. The deduction is done keeping in mind Ref. [10] when the PbI_2 platelets transform in rods belonging to another compound. An additional signature of the chemical intercalation mechanism is given of the modification of Raman spectrum of the guest. In this context, Fig. 4 shows a down-shift of the Raman lines of ANI from 1280 and 1602 cm^{-1} to 1224 and 1598 cm^{-1} and a change of the ratio between the intensities of Raman bands in the spectral ranges 950–1000 and 1550–1650 cm^{-1} from ca. ~1:1 to ca. 2:1. In this case, the interaction of ANI with PbI_2 involves the formation of new covalent coordinative bonds Pb–NH_2. This leads to the appearance of a positive charge on the nitrogen atom of ANI which is compensated by I^- ion. At the first sight, the association of the Raman band at 170 cm^{-1} with the presence of Pb–NH_2R (where $R = C_6H_5$) bond can be simply considered as speculative. Returning to the Fig. 3, the gradual increase in intensity of the Raman band at 170 cm^{-1} indicates that during of the electro-polymerization of ANI on the PbI_2 modified Pt electrode, new covalent bonds of the type Pb–NR_2 (where $R = C_6H_4$) between PANI-ES and PbI_2 appear. In other words, a PANI-ES/PbI_2 composite is formed. If this is correct, then the 170 cm^{-1} line must be observed differently in the Raman spectra of PANI-ES/PbI_2 and PANI-EB/PbI_2 compounds obtained by mechanico-chemical interaction as a result of a non-hydrostatic compression carried out at ca. 0.58 GPa for ca. 5 min. Relevant arguments are provided in Figs. 5 and 6. Fig. 5 shows the Raman spectra of PANI-EB, PANI-ES and PbI_2 mechanico-chemical intercalated with 5% and 10% PANI-EB. As for PANI-ES, the Raman spectrum of PANI-EB develops in the spectral range 1000–1650 cm^{-1}. According with Ref. [31] the main Raman lines of PANI-EB situated at ca. 1162, 1214, 1374, 1486 and 1594 $cm^{-1}$are associated with the C–H bending (Q)-Ag mode, C–N stretch. +ring def. (B)+C–H bending (B), C–C stretch. (Q)+C–H bending (B), C═N stretch. +C–H bending (B) and C–C stretch. (B)+C═C stretch. (Q) vibration modes, respectively. Two facts are important to be noticed in Fig. 5: (i) the absence of the Raman line at 170 cm^{-1} indicates that in the case of PANI-EB the vibration associated to the bond Pb-NHR_2, no longer exists; (ii) independent of the PANI-EB weight used for the mechanico-chemical interaction with PbI_2, the Raman spectra of the resulted composites (Fig. 5b and c) show in the spectral range 1000–1650 cm^{-1} vibrational features which belong to the PANI-ES. This experimental fact is a consequence of

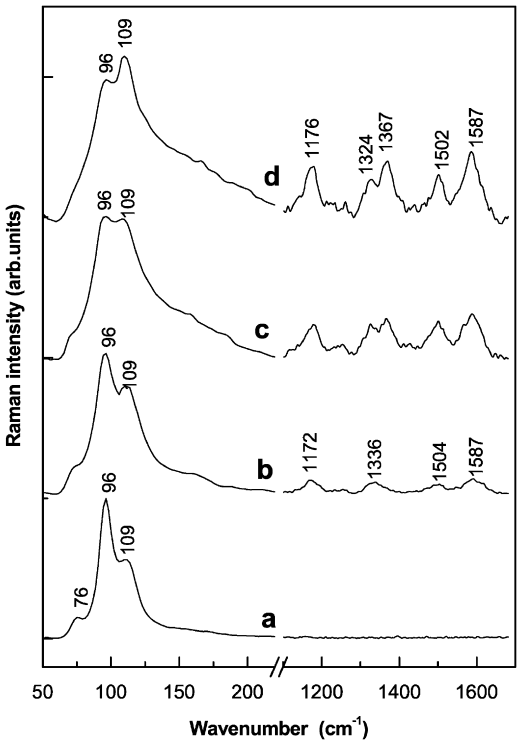

Fig. 5. Raman spectra of PANI-EB (a), PANI-ES (d) and the composites, obtained by mechanico-chemical reaction (non-hydrostatic compression at 0.58 GPa), of the type PbI_2/PANI-EB 5% (b) and PbI_2/PANI-EB 10% (c).

a charge transfer between the two constituents that is illustrated by the reaction presented in Scheme 2.

This suggests the formation of covalent coordinative bonds Pb–NR_2 in the macromolecular chain that explain the appearance in Fig. 5 of the PANI-ES signature noticed by an up-shift of the Raman bands at 1162 and 1486 cm^{-1} to 1170 and 1506 cm^{-1}, which are associated with the vibration mode C–H bending (Q) and C═N stretch. +C–H bending (B), respectively. On the other hand, the absence of the Raman line at 170 cm^{-1} must be correlated with the fact that the formation of new covalent coordinative bonds Pb-NHR_2, resulting from the addition of two macromolecular chains on the I–Pb–I layer is possible only if PANI-EB has been transformed in totality in PANI-ES. This reasoning is well supported by Fig. 6, which shows that increasing the PANI-ES weight in the polymer/PbI_2 mixture; one observes a gradual growth of the shoulder located in the Raman spectral range where there is the line at 170 cm^{-1}. For a better understanding of the interactions between PANI-ES and PbI_2 we propose a schematic diagram of the penetration of the polymer chains into the interlayers of PbI_2 as well as the molecular structure of the product noted as [$(PbI_2)_2$(PANI-$ES)_2$] (Scheme 3).

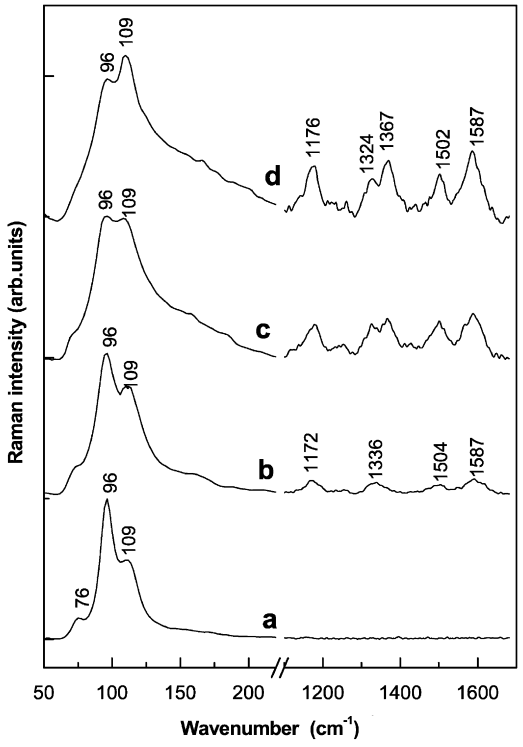

Fig. 6. Raman spectra of PbI_2 (a) and the PANI-ES/PbI_2 composites resulted from mechanico-chemical reaction (non-hydrostatic compression at 0.58 GPa), when PANI-ES concentrations of ca. 2% (b), 5% (c) and 10% (d) were used.

In this context one expects that the hybrid materials PANI-ES/PbI_2 and PANI-EB/PbI_2 must be characterized by different physical and chemical properties. Confirmation is obtained through PL studies.

PbI_2 crystal under band-to-band optical excitation shows a strong PL at LNT, Fig. 7. Three emission bands are detected: one at 2.495 eV originating from the radiative recombination of excitons, another at about 2.4 eV, noted as the D band, which strongly depends on the crystal quality and the third, labeled as the G band, formed by two components at about 2.06 and 1.86 eV coming from the radiative recombination of the trapped carriers [12]. The intensities of the G and D bands depend on the surface defects density and they enhance by thermal annealing and mechanical scratching of the crystal surface. The G and D bands originate from the radiative recombination of excitons and photocarriers trapped at the crystal surface. A supporting argument is the observation that they disappears after removal of the top layer of sample. As it is expected, the largest intensity of the G band is observed on the PbI_2 samples in form of crystalline powder. Thus, the Fig. 7B_2 and C_2 reveal a subtle variation of the excitation spectra of the G emission band. For the sample in form of crystal slide with surface defects induced mechanically, the Fig. 7B_2 discloses two peaks in the excitation spectrum of the G band, situated at 2.47 and 2.51 eV. The later coincides with a valence-band-to-conduction-band transition by which electric carriers (electrons and holes) are formed while the former indicates the formation of excitons. The crystalline powder behaves differently; it represents a situation in which the density of surface defects is

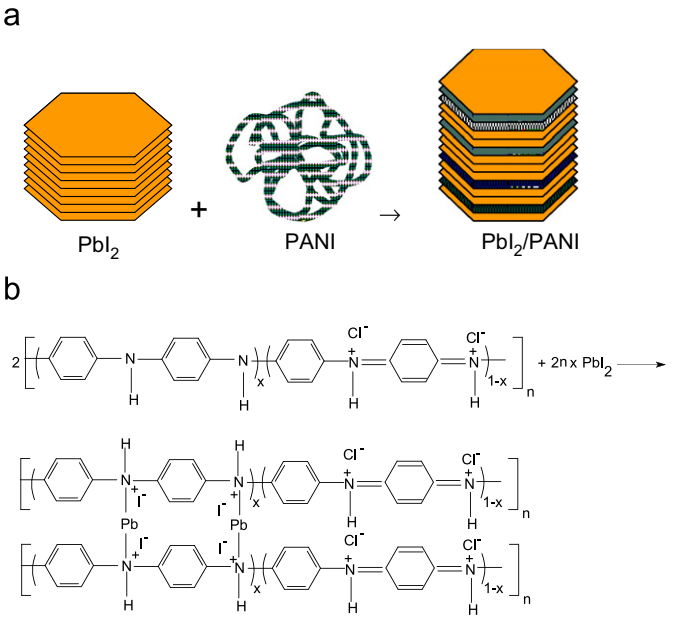

Scheme 3.

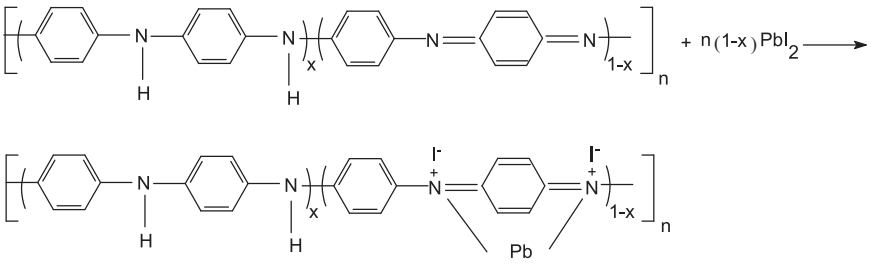

Scheme 2.

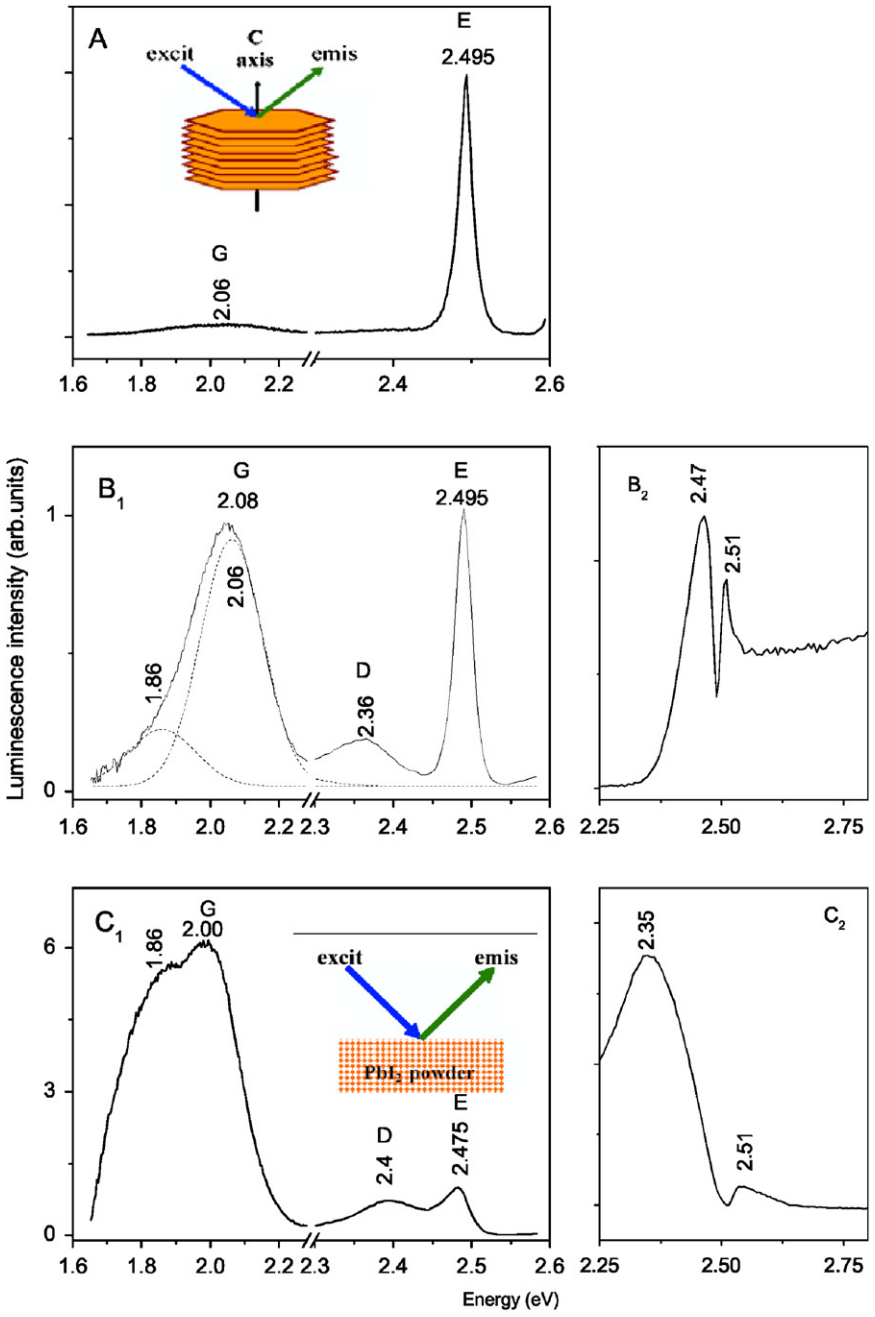

Fig. 7. (A) photoluminescence at LNT of a PbI_2 slice cleaved from an as grown crystal; (B) crystalline slide with surface defects produced mechanically; (C) PbI_2 microcrystalline powder. The corresponding excitation spectra of the G band are presented in figures (B_2) and (C_2).

the largest. In this case, the G band is accompanied by an intense D band at 2.34 eV, Fig. 7c_1. They appear also in the crystalline sample with a scratched surface as well as in PbI_2 powder, both cases being characterized by a "flaky" structure. Correlated studies of raman scattering and PL allow associating the D emission band with the presence of stacking faults induced in the layer structure of PbI_2. The Raman signature of stacking faults in the PbI_2 crystal is given by an additional line at 86 cm^{-1} [22,23]. It appears as a disruption of the continuous stacking of the I–Pb–I atomic planes along the *c* axis where the crystal point defects are accumulated. These defects are traps for the electrons and holes which by radiative recombination generate G band. A convincing result is presented in Fig. 7C_2 which shows that the most intense band in the excitation spectrum of the G band with the maximum at ~2.35 eV practically coincides with the position of the D emission band at 2.4 eV (Fig. 7C_1).

If the G band really originates from the radiative recombination of electrons and holes trapped at the crystal surface and stacking faults, it must present a particular variation changing the irradiation time and the exciting energy. The intensity of the G band depends on the number of trapped electrons and holes which recombine radiatively. If the sample is subjected to successive irradiations with light that provides a transition from the valence band to the conduction band, the number of carriers increases progressively. They diffuse in the mass of crystal and they are trapped on the defects from where by radioactive recombination gives rise to a G increasing band. A similar variation of the G band is expected if the energy of exciting light

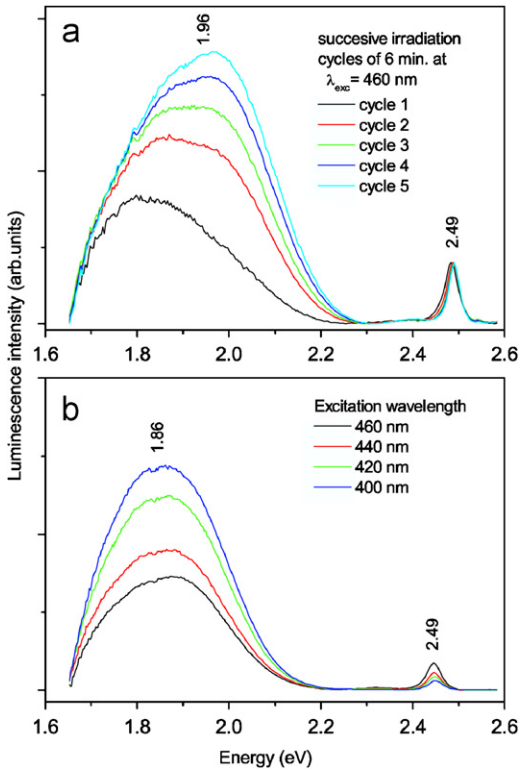

Fig. 8. photoluminescence at LNT of PbI_2 crystalline micrometric powder at $\lambda_{exc} = 460$ nm varying the irradiation time (a) and the energy of excitation light (b).

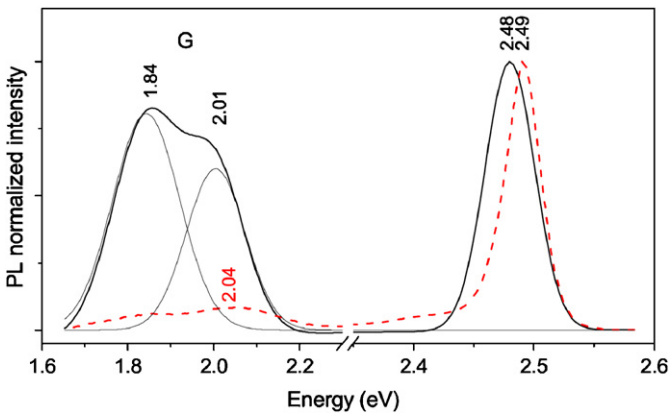

Fig. 9. Charges collector effect of PANI-ES electrochemically intercalated in PbI_2 single crystal evidenced by photoluminescence at LNT. Black spectrum corresponds to an as grown PbI2 crystalline sample and dashed spectrum is for PbI_2 intercalated with PANI-ES.

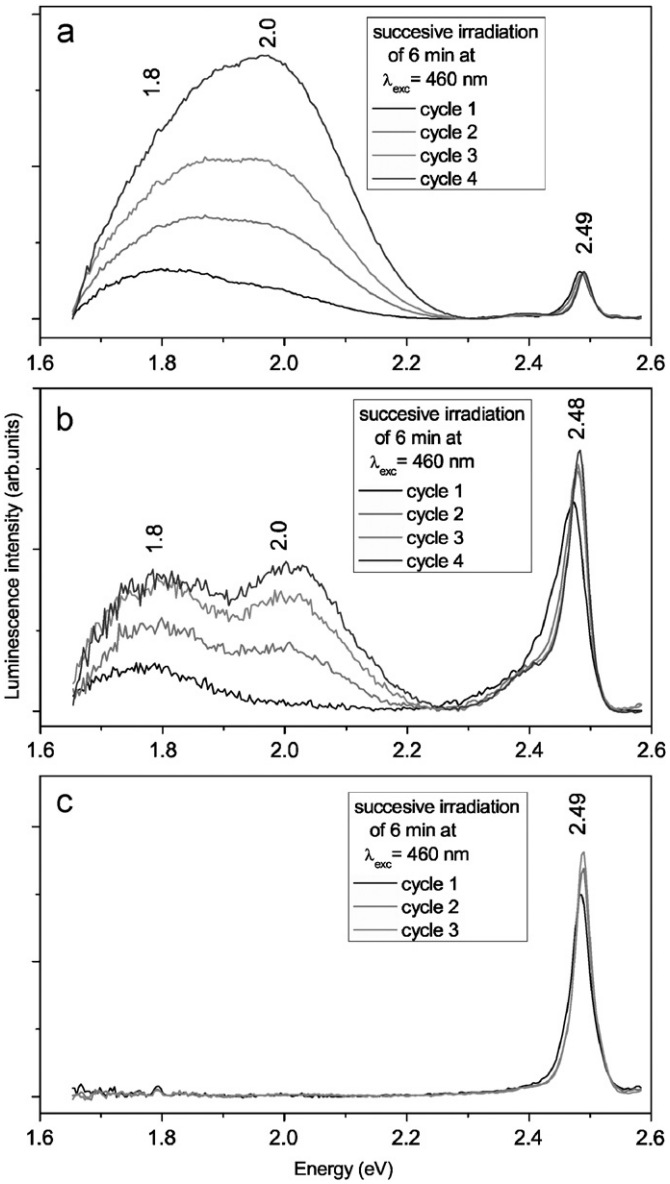

Fig. 10. Charges collector effect in PbI_2/PANI mechanico-chemical compound. photoluminescence at LNT of a PbI_2 crystalline micrometric powder (a), PbI_2/PANI-EB compound (b) and PbI_2/PANI-ES compound (c).

increases. In general, the PL of a semiconductor originates in radioactive processes occurring both at the surface and volume. The weight of each one depends on the penetration depth of the exciting light inside the crystal. The signature of the surface effects becomes dominant as the energy of the excitation light increases, i.e., when the exciting light is absorbed in the surface layers where are localized the largest density of traps. These considerations are sustained of Figs. 8a and b where one sees that the intensity of G band progressively increases both with the irradiation time and the energy of excitation light. The spectra presented in Fig. 8a were obtained after successive irradiations for 6 min at 460 nm; they illustrate the gradual growth of the number of trapped electrons and holes which afterwards by radioactive recombination generate G band. In this context, the question arises how the PL spectrum of a hybrid material of the type PANI/PbI_2, where PANI may be in the PANI-EB or PANI-ES form? The answer is obtained by investigating the PANI/PbI_2 compound prepared both electrochemically and mechanico-chemically. The relevant results are those shown in Figs. 9 and 10. Fig. 9 presents the PL spectrum at liquid nitrogen temperature of PbI_2 before and after electrochemical intercalation of PANI in the state of ES. Before intercalation the PL spectrum contains two strong emission band; one at 2.48 eV originating in the exciton recombination and another labeled G band with two components at about 2.01 and 1.84 eV due to the radiative recombination of trapped electrons and holes on the surface defects. The G band is very sensitive to a charge collection process that can appear if the PbI_2 crystal architecture is penetrated by conducting molecular structures. Indeed, such an effect is revealed in Fig. 9 by dashed spectrum obtained on PbI_2 intercalated electrochemically with PANI-ES. The decrease of G band argues the fact that a part carriers produced by the band-to-band excitation are collected by the conductive

materials that is PANI-ES. Fig. 9 discloses also a very subtle result. One observes that in the intercalated sample the excitonic emission band is shifted towards high energy. Intercalation of PANI-ES molecules disrupt the stacking sequence of layers in isolated packages of nanometric thickness alternating along the *c* axis in which different numbers of I–Pb–I layers are bound together. These structures, behaving as a quantum wells, will be perceived by the blue shift of the narrow excitonic emission band, fact that indicates a quantum confinement effect [23].

The same effect concerning the variation of the G band is clearly revealed by Fig. 10b and c which presents the PL of a crystalline powder of PbI_2 interacted mechanico-chemically with PANI in its two forms, PANI-EB and PANI-ES, respectively. The inciting fact is the appearance of a weaker G band when the PbI_2 has interacted mechano-chemically with PANI-EB and even its disappearance when the interaction has taken place with PANI-ES. The explanation is simple. PANI-ES is a conducting polymer, which interposed intimately between the PbI_2 particles, may play the role of a charge collector. The intimate term suggests that a suitable contact between PbI_2 particles and the polymer leads to a possible charge transfer. The mechanism proposed in this context is that charges formed by band-to-band irradiation, before their trapping on the crystal defects, are immediately collected by PANI in its conducting form, PANI-ES. Thus, in Fig. 10c the absence of G band can be explained by the radiative recombination of separately trapped carriers which no longer exist. Therefore, the presence of only one emission band (~2.49 eV) in the PL spectrum of PbI_2/PANI-ES hybrid materials is understandable. It comes from the exciton radiative recombination that is a coupled electron–hole pair bound together by a strong electrostatic attraction. Fig. 10b raises another question: why a diminished G band still appears in the PbI_2/PANI-EB mechanico-chemical compound, taking into account that PANI-EB is an insulator? By the use of an insulating polymer, would we obtain a behavior similar to that shown in Fig. 10a. The answer is found in Fig. 5 where one demonstrates by Raman spectroscopy that, from the mechanico-chemical interaction between PbI_2 and PANI-EB, a partially transformation of PANI-EB into PANI-ES took place.

4. Conclusions

In this work new results are reported concerning the synthesis and the vibrational and photoluminescence properties of the hybrid materials of the type PANI-ES/PbI_2 and PANI-EB/PbI_2. Our results leads to the following conclusions: (i) the electrochemical polymerization of aniline on the PbI_2 modified Pt electrode as well as mechanico-chemical reaction between the PANI-ES and PbI_2 leads to the formation of a PANI-ES/PbI_2 composite based on the covalent coordinative bonds of the type Pb-NHR_2, revealed in Raman spectrum by the line at ca. 170 cm^{-1}; (ii) the mechanico-chemical interaction between PANI-EB and PbI_2 involves a charge transfer between the two constituents which confer to PANI a salt character; (iii) photoluminescence studies reveal for the unreacted PbI_2, two main emission bands at ~ 2.49 and ~2.00 eV (G band) originating in the radiative recombination of excitons and trapped electrons and holes, respectively. The surface defects are primarily involved in the PL emission and this fact is demonstrated by a specific variation of the G emission band with the irradiation time and the energy of excitation light and (iv) a collecting charge process has been evidenced for the first time as occurring at the interface of the two constituents of the PANI-ES/PbI_2 composite.

Acknowledgments

Authors thank to Dr. Nicoleta Preda for producing and supplying Fig. 1. This work was performed in the framework of the scientific cooperation between the Institute of Materials "Jean Rouxel", Nantes, France, and the Laboratory of Optics and Spectroscopy of the National Institute of Materials Physics, Bucharest, Romania. This research was financed by the Romanian National Authority for Scientific Research as project Nr. 2-CEx-06-11-19/25.07.06.

References

[1] M. Baibarac, P. Gomez-Romero, J. Nanosci. Nanotechnol. 6 (2006) 289.
[2] A. Tiwari, A.P. Mishra, S.R. Dhakate, R. Khan, S.K. Shukla, Mater. Lett. 61 (2007) 4587.
[3] K. Mallick, M.J. Witcomb, R. Erasmus, M.S. Scurrell, Mater. Sci. Eng. B 140 (2007) 1663.
[4] C.B. Jing, J.X. Hou, J. Appl. Polym. Sci. 105 (2) (2007) 697.
[5] I. Boyano, M. Bengoechea, I. de Meatza, O. Miguel, I. Cantero, E. Ochoteco, J. Rodrýguez, M. Lira-Cantu, P. Gomez-Romero, J. Power Sources 166 (2007) 471.
[6] C. Wei, Y. Zhu, X. Yang, C. Li, Mater. Sci. Eng. B 137 (2007) 213.
[7] L.J.A. Koster, W.J. van Strien, W.J.E. Beek, et al., Adv. Funct. Mater. 17 (2007) 1297.
[8] M.R. Tubbs, Phys. Status Solidi B 49 (1972) 11.
[9] C.J. Sandroff, S.P. Kelty, D.M. Hwang, J. Chem. Phys. 85 (1986) 5337.
[10] M. Baibarac, N. Preda, L. Mihut, I. Baltog, S. Lefrant, J.Y. Mevellec, J. Phys. Condens. Matter 16 (2004) 2345.
[11] C.C. Coleman, H. Goldwhite, W. Tikkanen, Chem. Mater. 10 (1998) 2794.
[12] N. Preda, N.L. Mihut, M. baibarac, I. Baltog, S. Lefrant, J. Phys.: Condens. Mater 18 (2006) 8899.
[13] R. Al-Jishi, C.C. Coleman, S. Treece, H. Goldwhite, Phys. Rev. B 39 (1989) 4862.
[14] L.C. Yu-Hallada, A.H. Francis, J. Phys. Chem. 94 (1990) 7518.
[15] N. Preda, L. Mihut, M. Baibarac, M. Husanu, C. Bucur, I. Baltog, J. Optoelectron. Adv. Mater. 10 (2008) 319.
[16] V. Mehrotra, S. Lombardo, M.O. Thompson, E.P. Giannelis, Phys. Rev. B 44 (1991) 5786.
[17] R.F. Warren, W.Y. Liang, J. Phys.: Condens. Matter 5 (1993) 6407.
[18] G.I. Gurina, K.V. Savchenco, J. Photochem. Photobiol. A 86 (1995) 81.
[19] I. Warf, T Gramstad, R. Makhija, M. Onyszchuk, Can. J. Chem. 54 (1976) 3430.
[20] T.A. Babushkina, T.P. Klimova, L.D. Kvacheva, S.I. Kuznetsov, Hyperfine Interact. 159 (2004) 43.
[21] N. Preda, L. Mihut, M. Baibarac, M. Husanu, C. Bucur, I. Baltog, J. Optoelectron. Adv. Mater. 10 (2008) 319.
[22] N.A. Davydova, J. Baran, M.K. Marchewka, H. Ratajczak, J. Mol. Struct. 404 (1997) 163.
[23] I. Baltog, M. Baibarac, S. Lefrant, J. Phys.: Condens. Matter 21 (2009) 025507.
[24] K.E. Drexler, Nanosystems: Molecular Machinery Manufacturing and Computation, Wiley, New York, 1992.
[25] M.A. Rodrigues, M.A. de Paoli, M. Mastragostino, Electrochim. Acta 36 (1991) 2143.
[26] R. Zallen, M.L. Slade, Solid State Commun. 17 (1975) 1561.
[27] M. Baibarac, L. Louarn, L. Mihut, S. Lefrant, I. Baltog, J. Polym Sci.: Part B: Polym. Phys. 38 (2000) 2599.
[28] W.S. Huang, B.D. Humphrey, A.G. MacDiarmid, J. Chem. Soc. Faraday Trans. 82 (1986) 2385.
[29] A. Sengupta, K.C. Mandal, J.Z. Zhang, J. Phys. Chem. B 104 (2000) 9396.
[30] W.K. Sears, M.L. Klein, J.A. Morrison, Phys. Rev. B 19 (1979) 2305.
[31] S. Quillard, G. Louarn, S. Lefrant, A.G. MacDiarmid, Phys. Rev. B 50 (1994) 12496.
[32] A.K. Rai, S. Kumar, A. Rai, Vib. Spectrosc. 42 (2006) 397.